Received: 25 July 2024 | Accepted: 6 November 2024

DOI: 10.1002/aps3.11628

APPLICATION ARTICLE

Applications in Plant Sciences

Microbial methods matter: Identifying discrepancies between microbiome denoising pipelines using a leaf biofilm taphonomic dataset

Brianne Palmer[1] | **Sabina Karačić**[2] | **Gabriele Bierbaum**[2] | **Carole T. Gee**[1]

[1]Division of Paleontology, Bonn Institute of Organismic Biology, Nussallee 8, 53115 Bonn, Germany

[2]Institute of Medical Microbiology, Immunology and Parasitology, University Clinic of Bonn, University of Bonn, Venusberg-Campus 1, 53127 Bonn, Germany

Correspondence

Brianne Palmer, Bonn Institute of Organismic Biology, Division of Paleontology, University of Bonn, Nussallee 8, 53115 Bonn, Germany.
Email: bpalmer@uni-bonn.de

Carole T. Gee, Bonn Institute of Organismic Biology, Division of Paleontology, University of Bonn, Nussallee 8, 53115 Bonn, Germany.
Email: cgee@uni-bonn.de

Abstract

Premise: The occurrence of different microorganisms on aquatic macrophyte fossils suggests that biofilm microbes may facilitate leaf preservation. Understanding the impact of microorganisms on leaf preservation requires studies on living plants coupled with microbial amplicon sequencing. Choosing the most suitable bioinformatic pipeline is pivotal to accurate data interpretation, as it can lead to considerably different estimations of microbial community composition.

Methods: We analyze biofilms from floating and submerged leaves of *Nymphaea alba* and *Nuphar lutea* and mock communities using primers for the 16S ribosomal RNA (rRNA), 18S rRNA, and ITS amplicon regions and compare the microbial community compositions derived from three bioinformatic pipelines: DADA2, Deblur, and UNOISE.

Results: The choice of denoiser alters the total number of sequences identified and differs in the identified taxa. Results from all three denoising pipelines show that the leaf microbial communities differed between depths and that the effect of the environment varied depending on the amplicon region.

Discussion: Considering the performance of denoising algorithms and the identification of amplicon sequence variants (ASVs), we recommend DADA2 for analyzing 16S rRNA and 18S rRNA. For the ITS region, the choice is more nuanced, as Deblur identified the most ASVs and was compositionally similar to DADA2.

KEYWORDS

amplicon sequencing, bioinformatics, denoising, leaf biofilms, plant taphonomy

Microbial sequencing is becoming increasingly integrated into interdisciplinary studies. In particular, there is growing interest in high-throughput sequencing in the interdisciplinary field of taphonomy, the study of how organisms decay and ultimately fossilize (Gee, 1996; Raff et al., 2008; Janssen et al., 2022; Dhami et al., 2023). Decay experiments, which have been more recently coupled with microbial assays, are being used to understand the role of biofilms in the decay of animals (Iniesto et al., 2017, 2021; Mähler et al., 2023) and plants (Iniesto et al., 2018; Janssen et al., 2021; Karačić et al., 2024), highlighting the important role of this approach in interdisciplinary research.

Using amplicon sequencing to assess the microbial community composition of biofilms in early decay experiments is a new technique used by experimental plant taphonomists to understand the role of biofilms in leaf decay and preservation (Janssen et al., 2021; Karačić et al., 2024). Biofilms comprise a matrix of microorganisms (e.g., bacteria, fungi, and algae) and their extracellular polymeric substances (EPSs) (Donlan, 2002). They form in a variety of natural environments, including surfaces in the water such as plant roots and the leaf surfaces of aquatic plants (Donlan, 2002; Pang et al., 2016). Plant leaves provide a unique habitat for biofilms as they can release oxygen via

cellular respiration, thus promoting the growth of aerobic bacteria (Lear et al., 2012). There are complex interactions between the plant leaf and biofilm, resulting in different microbial communities within the biofilm as compared to those in the surrounding water column (He et al., 2014). Plants that are completely submerged experience differences in water flow, light conditions, and nutrient concentrations compared to floating freshwater plants (He et al., 2012). Biofilms commonly lead to the degradation of plant tissue, especially in eutrophic waters (Dong et al., 2017). The presence of biofilms can ultimately lead to the degradation of living leaves by the blocking of light, which prohibits photosynthesis, and biofilm organisms may compete with the host plant for resources such as light and nutrients (Letáková et al., 2018). However, degradation of plant tissues by biofilms does not always occur.

In some aquatic environments, biofilms can be important for the preservation of tissues. Previous research has emphasized the importance of biofilms for the fossilization of both soft-bodied and mineralized body parts and soft tissue associated with dinosaur bones (Kaye et al., 2008; Peterson et al., 2010), embryos (Raff et al., 2008), tadpoles (Toporski et al., 2002), and crayfish (Mähler et al., 2022) based on experimental taphonomy and the imaging of well-preserved fossil tissues. Furthermore, there is evidence that microbial biofilms are also involved in the long-term preservation of plant tissue (Iniesto et al., 2018). Recently, Karačić et al. (2024) found changes in the community composition of leaf biofilms under aerobic and anaerobic conditions using amplicon sequencing, highlighting the role of environmental conditions in leaf preservation and decay.

However, the results of such microbiome studies are vulnerable to biases due to differences in bioinformatic pipelines (Allali et al., 2017; Prodan et al., 2020). Thus, there is a need to define best practices for microbial community studies in microbial taphonomy, particularly regarding plant studies. Using environmental plant biofilms from two genera of water lilies (Nymphaeaceae) and mock communities, we aim here to assess the differences in three common pipelines (DADA2, Deblur, and UNOISE) and describe the biases introduced through each pipeline. Similar analyses have been performed previously (Nearing et al., 2018; Prodan et al., 2020; Nilsen et al., 2024). However, when working with environmental data from different environments, the effectiveness of the denoising pipelines can vary. Nearing et al. (2018) found that DADA2 identified more amplicon sequence variants (ASVs) than Deblur and UNOISE, whereas Nilsen et al. (2024) found that UNOISE had the greatest ASV richness and outperformed Deblur and DADA2 when using high-diversity seafloor samples. Furthermore, using a fecal dataset, Prodan et al. (2020) found that DADA2 offered the best sensitivity with less specificity and suggested that UNOISE reached a balance of sensitivity and specificity. Therefore, it is highly important to explore different bioinformatic pipelines for specific types of samples of interest to better understand their biases. Providing an overview of results from different pipelines facilitates a better understanding of microbial community results and their function in the environment.

Because biofilms are diverse communities of microorganisms living in a variety of different environments, they are an ideal community to study the effectiveness of denoising pipelines in an environmental context. Furthermore, this analysis is the first, to our knowledge, to identify the effectiveness of these pipelines using 16S, ITS, and 18S datasets collected from the same samples.

METHODS

Sample collection

In July 2022, six leaves of *Nymphaea alba* L. and six leaves of *Nuphar lutea* (L.) Sm. were collected from the largest pond lined with *Taxodium* Rich. at the University of Bonn Botanical Garden in Bonn, Germany. Half of the leaves were floating, and the other half were submerged in the pond sediment. The pond is in an urban environment with a community of aquatic plants and animals that is replenished by rainfall and a small stream. In the month before sample collection, the mean water temperature was 18.4°C. Among the floating leaves, brown leaves with signs of biofilm development were preferentially selected. The leaf biofilms were identified visually, and leaves with a thick, mucous-like coating were selected. The biofilm was distinguishable from water, as it did not fall off the leaf when gently shaken. The submerged leaves were settled on the bottom of the pond beneath the mud and had likely been there since the previous winter (~6 mo), although the exact duration of the leaf decay is unknown. The submerged leaves were no longer attached to their respective parent plants by a petiole.

The three floating leaves each of *Nymphaea* and *Nuphar* were placed into separate bins containing water from the pond. To reduce further contamination, the bins had been cleaned previously with ethanol. The submerged leaves of each plant species were collected from pond mud at a water depth of approximately 1 m and immediately placed in a separate bin filled with pond water. Neither the floating nor submerged leaves were rinsed or washed to ensure the biofilms stayed intact. Pond water and pond sediment were collected in triplicate in sterile 50-mL Falcon tubes on the same day. The pond water was removed from the surface of the pond, and the pond sediment was collected directly from where the water lily leaves were submerged. Sequencing of the pond water and sediment samples provides information about the microbes present in the environments to which the biofilms were exposed.

DNA extraction and sequencing

Leaves were stored in Tris-EDTA (TE) buffer at −20°C for DNA extraction. To separate the biofilm from leaf surfaces, the leaves stored in TE buffer were thawed and then

sonicated in an ultrasound bath (Branson 1210 Ultrasonic Cleaner; Emerson, St. Louis, Missouri, USA) for 2 min. After sonication, the samples were first filtered through a sterilized coarse filter (grade: 3hw; Binzer & Munktell Filter, Battenberg, Germany) to remove leaf debris and sediment. The filtrated samples were filtered a second time using vacuum filtration and a 0.20-µm pore filter (mixed cellulose ester membrane; Berrytec, Grünwald, Germany) to retain the bacteria, fungi, and algae. These filters were stored in 50-mL Falcon tubes at −20°C until DNA extraction.

The DNA from the filters was extracted using the FastDNA Spin Kit for Soil (MP Biomedicals, Irvine, California, USA), which had been tested by our working group and found to be optimal for leaves in our freshwater environmental setting (Janssen et al., 2021). Previous studies have shown this kit's effectiveness in extracting DNA from waterlogged sediment and freshwater (Knauth et al., 2013; Lee et al., 2021). The extractions were performed following the manufacturer's instructions, and the DNA was eluted in 50-µL DNase-free water. DNA concentration and quality were checked using a NanoDrop One/OneC Microvolume UV-VIS spectrophotometer (Thermo Fisher Scientific, Waltham, Massachusetts, USA).

High-throughput amplicon sequencing was performed using three sets of primers to capture the diversity of bacteria (16S ribosomal RNA [rRNA]), fungi (ITS region), and diatoms (18S rRNA). For 16S rRNA sequencing, we used the V4 variable region using the F515 (GTGYCAGCMGCCGCGGTAA) and R806 (GGACTACVSGGGTATCTAAT) primers (Caporaso et al., 2011). The V1 and V2 regions of the 18S rRNA gene were amplified using SSU_F04 (GCTTGTCTCAAAGATTAAGCC) and SSU_R22 (GCCTGCTGCCTTCCTTGGA) primers (Choi et al., 2022). The ITS rRNA region was amplified using the ITS-1F (CTTGGTCATTTAGAGGAAGTAA) and ITS-2R (GCTGCGTTCTTCATCGATGC) primers (Korabecná et al., 2003). Soil and water samples were sequenced in triplicate for only 16S and ITS. The PCR reaction was a single-step PCR with HotStarTaq Plus Master Mix Kit (QIAGEN, Hilden, Germany) The initial denaturation lasted 5 min at 95°C followed by 95°C for 30 s, 53°C for 40 s, and 72°C for 1 min for 30–35 cycles. The final elongation step was at 72°C for 10 min. Paired-end sequencing (bTEFAP) was performed by MR DNA (Shallowater, Texas, USA; http://www.mrdnalab.com) on the MiSeq sequencing platform (Illumina, San Diego, California, USA) with 2 × 300 paired-end reads following the manufacturer's guidelines (Dowd et al., 2008). All sequences and raw data are available through the National Center for Biotechnology Information (NCBI) under BioProject number PRJNA1043867 (http://www.ncbi.nlm.nih.gov/bioproject/1043867).

Mock communities

Mock communities representing the 16S rRNA, ITS, and 18S rRNA regions were chosen from previous studies. Janssen et al. (2021) had previously used the 16S rRNA mock community to test the effectiveness of DNA extraction kits using the 16s-515F (GTGCCAGCMGCCGCGGTAA) and 16s-806R (GGACTACVSGGGTATCTAAT) primers. All sequences were deposited in the European Nucleotide Archive (study accession number 471 PRJEB43756). The ITS region mock community was developed by Bakker (2018) using the ITS-1 (CTTGGTCATTTAGAGGAAGTAA) and ITS-2 (GCTGCGTTCTTCATCGATGC) primers. The mock community sequences with even amounts of each community member and unmodified PCR conditions were chosen for this study and downloaded from the NCBI database under BioProject number PRJNA377530. The 18S mock community was originally developed in Bradley et al. (2016) using the EukA (AACCTGGTTGATCCTGCCAGT) and EukB (TGATCCTTCTGCAGGTTCACCTAC) primers. All sequences are deposited in the NCBI Database under BioProject number PRJNA314977.

Pipelines and parameters

Three different pipelines were tested: DADA2 (Callahan et al., 2016), Deblur (Amir et al., 2017), and UNOISE (Edgar, 2016). We aimed to compare the pipelines with these typical conditions to match the most plausible use. All steps in the DADA2 and Deblur pipelines were performed in QIIME2 (qiime2-amplicon-2023.9) (Bolyen et al., 2019) using Python 3.10.8. USEARCH/UNOISE was run within VSEARCH (Rognes et al., 2016) until taxonomic classification (Appendix S1; see Supporting Information with this article). At that point, all three pipelines were classified using the same databases. The Silva v138 database (Quast et al., 2013) was used for identification of 16S and 18S rRNA samples, and UNITE version 10.0 with 97% identity (Nilsson et al., 2019) was used to classify the ITS region. These bioinformatic processes take raw DNA sequences and use denoising programs to group the sequences into ASVs representing the microbial members identified, which can then be linked with taxonomic databases to provide information on the composition of the communities.

DADA2

DADA2 begins by building an error model based on the distribution of errors observed in the sequencing data (Callahan et al., 2016) (Appendix S1); this includes both substitution errors and insertion/deletion errors. The DADA2 denoise pipeline (*dada2 denoise-paired*) was run with a minimum trim length of 230 bp (Appendix S2). The reads were dereplicated, which collapses all the reads that code for the same sequence. Unique to DADA2 is the algorithm that learns the error rates introduced by PCR amplification and sequencing based on a subset of the data. This is followed by sample inference, which uses another algorithm to infer ASVs. Up to this point, all processes were performed separately on forward and reverse reads;

the reads were then merged and the chimeras removed (Appendix S1).

Deblur

Unlike DADA2, Deblur uses only forward reads (Amir et al., 2017). We used the Deblur pipeline within QIIME2 (*deblur denoise-16S* for bacteria and *deblur denoise-other* for fungi and eukaryotes) with a minimum trim length of 230 bp. Similar to DADA2, Deblur collapses identical sequences into unique representatives and uses an error model to estimate the error rates in the sequencing data. The denoising process in Deblur involves clustering similar sequences together and constructing consensus sequences. The algorithm uses the error model to identify and correct errors, resulting in the generation of high-quality, denoised sequences. This is followed by chimera detection and removal, and as in DADA2, an ASV table is then generated with abundances assigned to each unique sample (Appendices S1 and S2).

UNOISE

UNOISE is not an open-source program; however, by using VSEARCH, we could use the UNOISE algorithm (Edgar, 2016) within QIIME2 and directly compare it to DADA2 and Deblur, which is also coded within QIIME2. The code for this process was derived from https://www.nicholas-ollberding.com/post/denoising-16s-sequence-reads-using-unoise3-via-vsearch-and-qiime2/. Like DADA2, this pipeline uses merged reads, which were filtered to a minimum length of 230 bp. VSEARCH was run within the QIIME2 environment and included the following steps: filtering low-quality reads, finding unique reads through dereplication, creating zero-radius operational taxonomic units (zOTUS) (analogous to ASVs) using *cluster_unoise*, removing chimeras, and mapping the reads back to centroids using *usearch_global*. The *cluster_unoise* command uses the UNOISE algorithm, which orders the sequences by decreasing abundance and removes sequences with fewer than eight counts (default threshold). It then uses a model on each sequence to compare its abundance with the abundance of its closest sequence. If the input sequence is less than 97% identical to its closest sequence, the input sequence becomes a new ASV. The *usearch_global* command searches for high-identity hits (97%) using the USEARCH algorithm (Appendices S1 and S2).

Taxonomic identification

After each denoising pipeline, the ASV tables were converted into QIIME2 objects for downstream taxonomic identification. Each dataset was assigned taxonomy using the *classify-consensus-vsearch* command and the Silva v138 (Quast et al., 2013) for the 16S rRNA and 18S rRNA regions and UNITE (qiime_ver10_97) (Nilsson et al., 2019) for the ITS region. For downstream statistical analyses, singletons were removed. Taxonomic tables were filtered in R so the 16S rRNA only contained ASVs classified as bacteria or archaea, ITS rRNA contained only fungi, and 18S rRNA contained nonfungal eukaryotes. This insured the datasets only included taxa with known domains and removed potentially contaminated ASVs. For each dataset, the taxonomic tables and ASV tables were merged using R to create one data frame.

Statistical analyses

Statistical analyses were performed in R (version 4.4.0; R Core Team, 2024). To determine differences in the effectiveness between pipelines, we compared the ASV richness (alpha diversity) using the *amp_alpha_diversity* function in the package ampvis2 (Andersen et al., 2018). For the mock communities, differences in the total number of ASVs and differences in the relative abundance of each genus identified by each pipeline were determined with ANOVAs.

The data were rarified to the smallest number of reads in any sample, resulting in 40,000 for 16S, 165 for ITS, and 15,620 for 18S. Differences in ASV richness between each pipeline were determined with ANOVAs. This analysis was performed with all the data from each pipeline and separately for each experimental environment (floating, submerged, water, and sediment) to determine if there were different effects of pipeline use depending on the environment. The number of shared genera was visualized with Venn diagrams (Liu et al., 2021). The differences in the community composition at the ASV level were measured with a permutational multivariate ANOVA (PERMANOVA) based on Bray–Curtis distances using the microeco package (Liu et al., 2021). These results were visualized using clustered bar plots, heatmaps, and principal coordinate analysis (PCoA) plots created with ampvis2 and microeco (Andersen et al., 2018; Liu et al., 2021). Differences in the identified phyla by each pipeline were assessed with ANOVAs.

RESULTS

Differences in 16S rRNA ASV richness and abundant genera among pipelines

The choice of pipeline alters the results of the mock community because it significantly impacts the total number of sequences identified ($F_{2,3219} = 58.3$, $P < 0.001$). DADA2 had the most sequences and UNOISE had the fewest (Appendix S3A). This is also evident in the total number of sequences assigned to each of the genera in the mock community (Appendix S3B). Thus, similar results were expected with the environmental samples.

There were differences in the total number of observed ASVs and the number of reads among pipelines, with

UNOISE detecting the most reads (Appendices S4 and S5). After removing ASVs with no taxonomic information (unidentified to domain or phylum), UNOISE had the greatest ASV richness (10,069) followed by DADA2 (8226) and Deblur (3634) in the biofilm samples ($F_{2,51} = 16.02$, $P < 0.0001$; Appendix S5). This differed from the mock community, in which UNOISE detected the fewest number of sequences. UNOISE had a greater Shannon diversity ($F_{2,51} = 7.6$, $P = 0.013$; Appendix S5). The pipelines only shared 515 (48.3%) genera in the biofilm samples, and DADA2 had the greatest number of unique genera ($n = 295$; Figure 1B). The relative abundance of each phylum was similar among pipelines, with Gammaproteobacteria and Alphaproteobacteria being the most dominant classes (Figure 1C). However, Alphaproteobacteria abundance varied among pipelines ($F_{2,51} = 12$, $P = 0.0005$), with UNOISE detecting the most Alphaproteobacteria sequences. There were differences in the relative abundance of microbial classes among environments, primarily between the surrounding environment (water and soil) and the biofilms. The water contained the most Gammaproteobacteria ($F_{3,50} = 50.03$, $P < 0.001$) and Bacteroides ($F_{3,50} = 50.12$, $P < 0.001$), whereas the soil contained more Alphaproteobacteria ($F_{3,50} = 8.7$, $P < 0.001$) and Verrucomicrobiae ($F_{3,50} = 60.64$, $P < 0.001$) compared to the other environments. The water also contained more Actinobacteria ($F_{3,50} = 24.5$, $P < 0.001$) compared to the biofilms, whereas the floating leaf biofilms contained more Cyanobacteria compared to the water ($F_{3,50} = 3.7$, $P = 0.015$).

The most dominant genera included *Rhizobium*, unidentified Cyanobacteria, *Pseudomonas*, *Nevskia*, *Limnohabitans*, *Novosphingobium*, *Pantoea*, and *Sphingomonas*; *Rhizobium* was the most prevalent across all leaves. DADA2, Deblur, and UNOISE each identified a different abundant Cyanobacteria ASV. *Pseudomonas* was more abundant on the submerged leaves, *Nevskia* and *Limnohabitans* were most abundant in the water samples, and *Novosphingobium* and *Pantoea* were more abundant in the biofilm of the floating leaves. The microbial community heatmaps resemble each other regardless of which pipeline

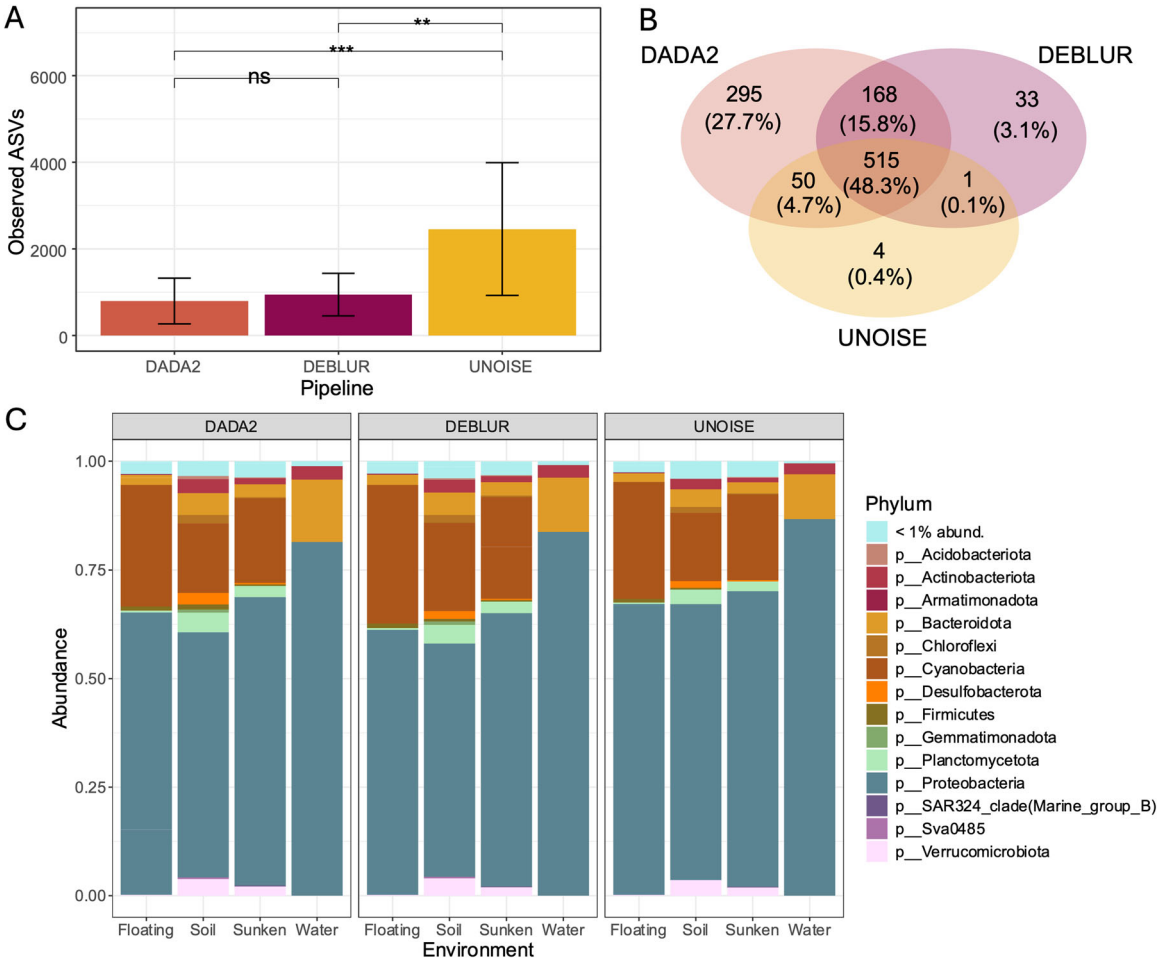

FIGURE 1 Alpha diversity of bacterial communities. (A) Bacterial amplicon sequence variant (ASV) richness for each experimental condition as determined by each denoising pipeline. The height of the bar represents the mean, and the bars are the standard deviation. Statistical differences in the number of ASVs detected by each pipeline determined by a *t*-test are noted with ns ($P > 0.05$), ** ($P < 0.01$), and *** ($P < 0.001$). (B) Venn diagram showing the number (and percentage) of bacterial genera unique to each pipeline and shared among them. (C) Stacked-bar plot showing the relative abundance of bacterial phyla (p__) identified from each pipeline and environment.

was used (Figure 2B). The PCoA and PERMANOVA analyses indicated that the overall community composition differs among the pipelines ($F_{2,51} = 3.1$, $P < 0.001$) and varies significantly in accordance with the experimental environments ($F_{3,50} = 2.5$, $P < 0.001$) (Figure 2A).

The 16S number of ASVs (richness) of the biofilm communities of submerged leaves was higher than the richness of the biofilms on the floating leaves (Appendix S6), likely influenced by the sediment that contained the most ASVs. There was no difference in Shannon diversity between floating and submerged leaves (Appendix S6). Prokaryotic biofilm community composition varied significantly between leaf depths ($F_{1,10} = 2.4$, $P = 0.013$), although not between plant species ($F_{1,10} = 0.73$, $P = 0.602$; Appendix S6).

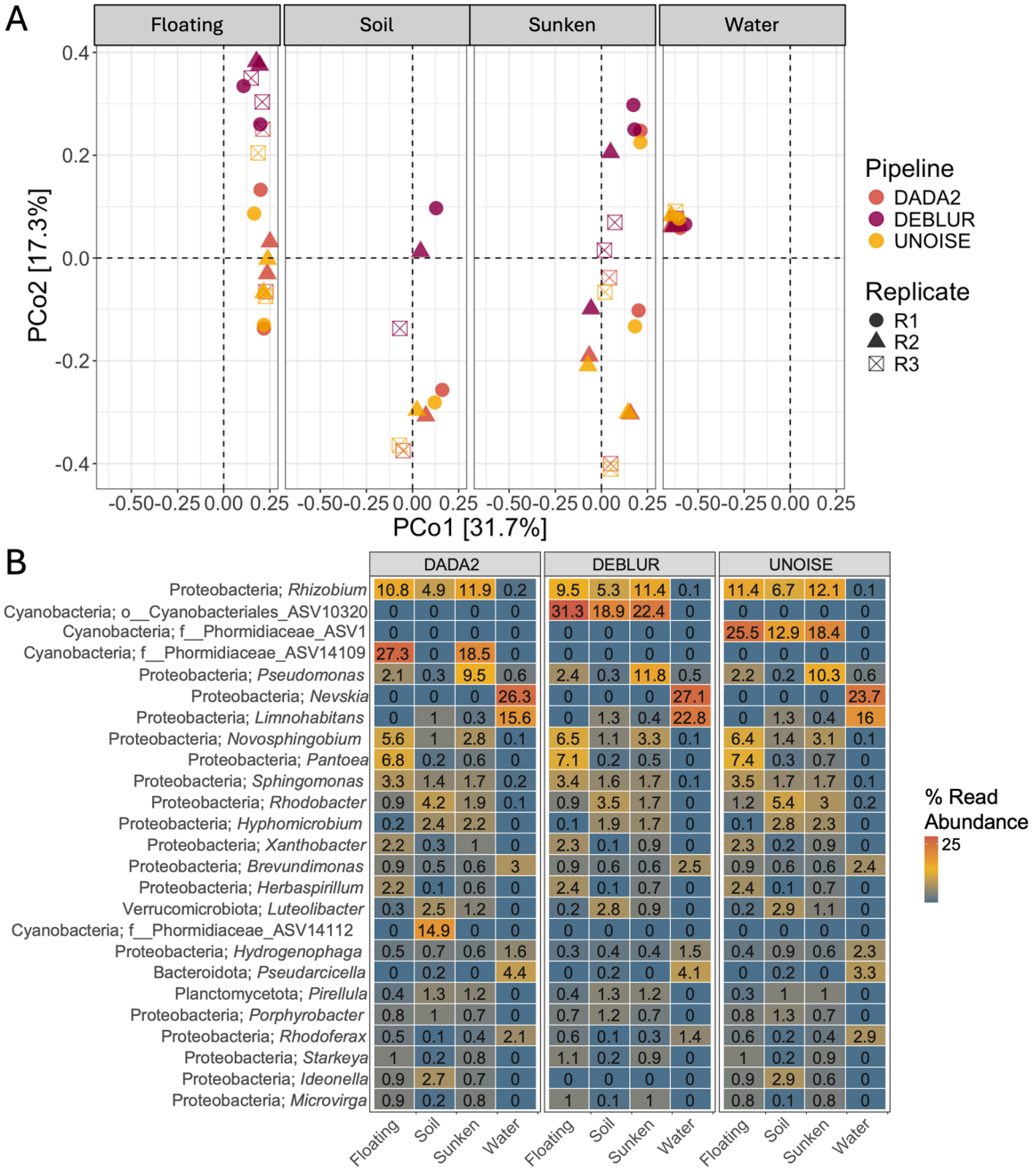

FIGURE 2 Bacterial microbial community composition. (A) Principal coordinate analysis (PCoA) plot of the bacteria community composition according to the experimental treatment. The colors represent the three pipelines, and the shapes represent the replicates. If the replicates from each pipeline are similar to each other, then they share a similar community composition. The *y*-axis is the same for each experimental condition and shows that the microbial community composition varied between floating and buried leaves. (B) Heatmap divided by the pipelines used showing the 25 most abundant genera with the experimental condition on the *x*-axis. Red squares indicate high abundance, whereas blue indicates lower abundance. When the genera were not known, the highest level of known classification is provided with the ASV number.

Significant differences in ITS region community composition among pipelines

Like the 16S analysis, the choice of pipeline for the mock community alters the total number of sequences identified ($F_{2,1017} = 8128$, $P < 0.001$). UNOISE identified the most sequences, whereas DADA2 and Deblur identified similar numbers of sequences (Appendix S3C). Although each pipeline identified the same genera, the relative abundance of the genera varied among the pipelines for the mock community (Appendix S3D). Such variation may also be expected with the environmental samples.

There were significant differences in the performance of the three pipelines in regard to the ITS rRNA sequences (Figure 3, Appendix S5). Based on the rarefaction curves, DADA2 best estimated the ASV richness (Appendix S4B). After the removal of ASVs with no domain or phylum information and after further filtering to only include fungi, Deblur ($n = 184$) detected significantly more ASVs than DADA2 ($n = 174$, $F_{2,51} = 7.2$, $P = 0.0024$) and UNOISE ($n = 98$, $F_{2,51} = 7.2$, $P = 0.011$) (Appendix S5). This differed from the mock community results, as Deblur detected more ASVs overall. In total, only 14.9% of genera were shared among all three pipelines, and 50% of the genera were unique to Deblur (Figure 3B). Even at the phylum level, there were discrepancies in the taxonomic identification, with Deblur identifying more Ascomycota ($F_{2,51} = 6.5$, $P = 0.003$) and UNOISE identifying more Basidiomycota, although this difference was not statistically significant ($F_{2,51} = 2.3$, $P = 0.11$; Figure 3C). There were differences in the relative abundance of each phylum based on the environment. The floating leaves contained more Ascomycota than the soil and water ($F_{2,51} = 6.5$, $P = 0.002$), whereas the water contained more *Mortierellomycota* ($F_{3,50} = 3.6$, $P = 0.019$), Mucoromycota ($F_{3,50} = 3.9$, $P = 0.013$), and Rozellomycota in DADA2 only ($F_{3,14} = 5.1$, $P = 0.013$).

There were also differences in the genera identified by each pipeline. *Plectosphaerella* was the most abundant genus identified by both DADA2 and Deblur, but not UNOISE. An unidentified fungus in Ceratobasidiaceae and *Saccharomyces* was abundant according to DADA2 and UNOISE, but not Deblur (Figure 4B). *Boeremia* was detected in high abundance with DADA2, whereas *Pyrenochaetopsis* was detected more frequently in Deblur (Figure 4B). The

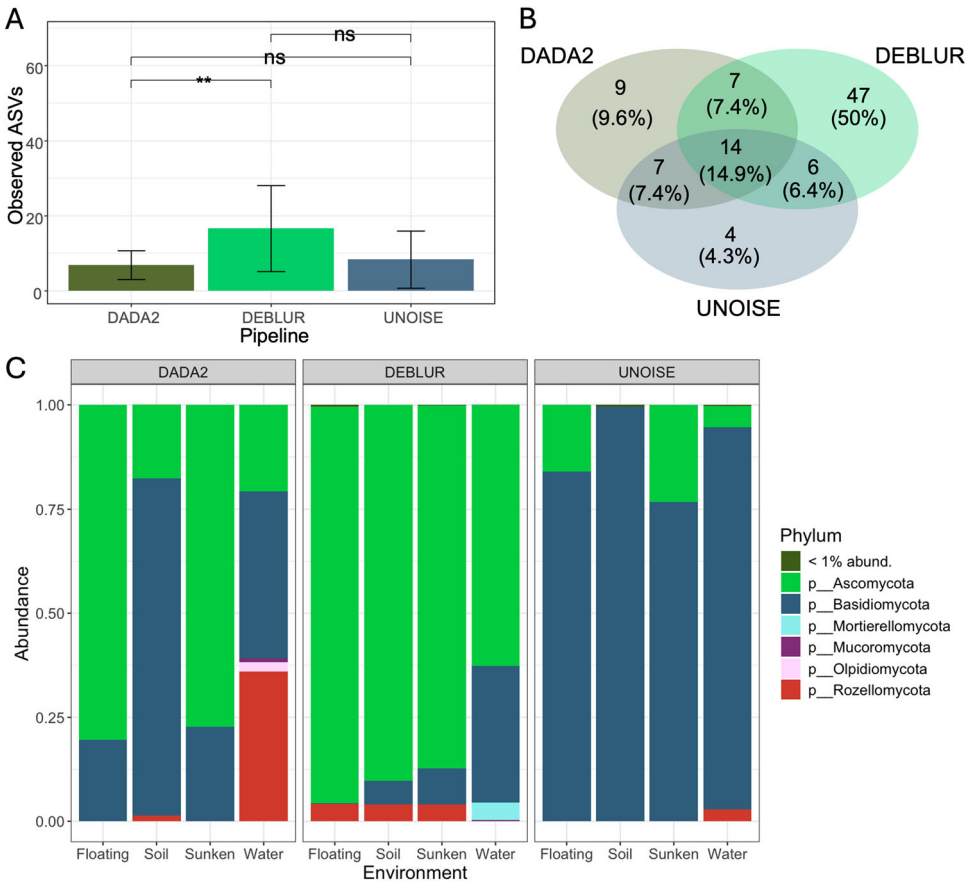

FIGURE 3 Alpha diversity of fungal communities. (A) Fungal ASV richness for each experimental condition as determined by each denoising pipeline. The height of the bar represents the mean, and the bars are the standard deviation. Statistical differences in the number of ASVs detected by each pipeline determined by a *t*-test are noted with ns ($P > 0.05$) and ** ($P < 0.01$). (B) Venn diagram showing the number (and percentage) of fungal genera unique to each pipeline and shared among them. (C) Stacked-bar plot showing the relative abundance of fungal phyla (p__) identified from each pipeline and environment.

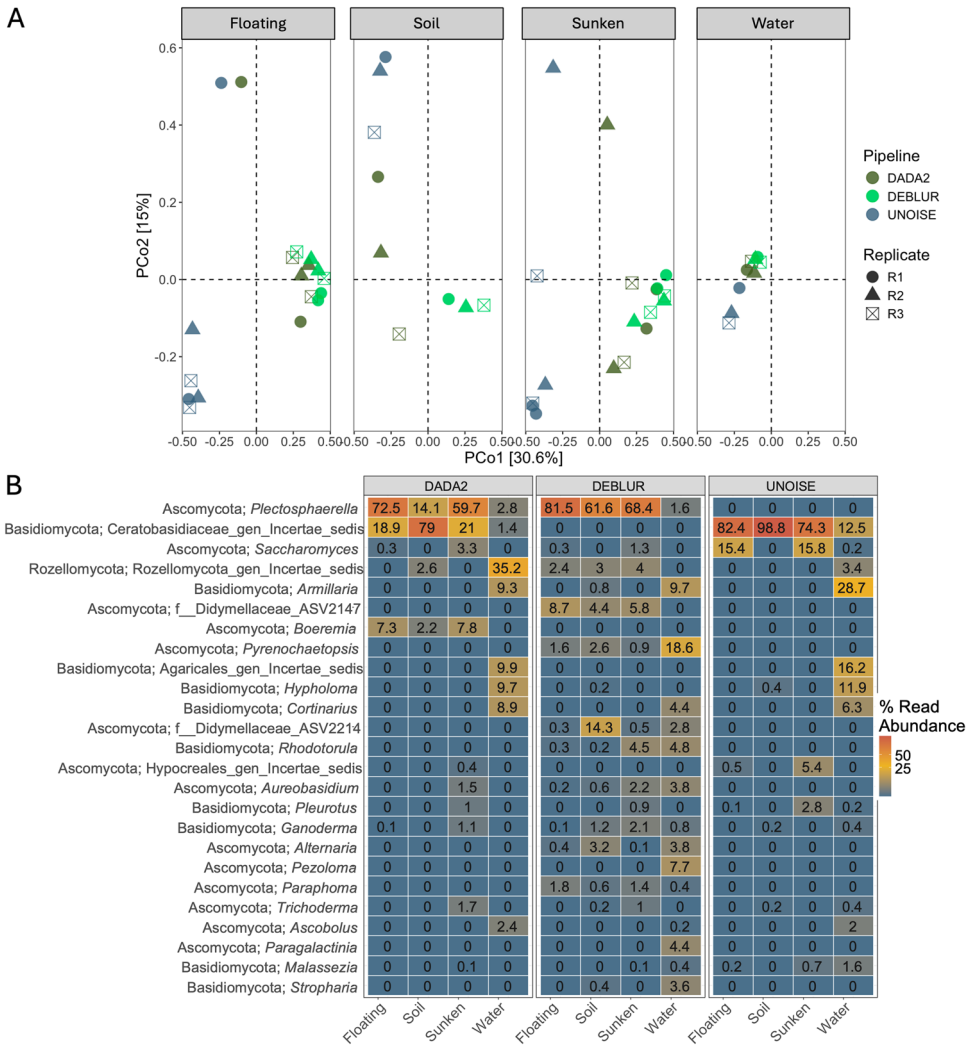

FIGURE 4 Fungal microbial community composition. (A) PCoA plot of the fungal community composition according to the experimental treatment. The colors represent the three pipelines, and the shapes represent the replicates. If the replicates from each pipeline are similar to each other, then they share a similar community composition. The *y*-axis is the same for each experimental condition and shows that the microbial community composition varied between *Nymphaea* and *Nuphar* leaves. (B) Heatmap divided by the pipelines used showing the 25 most abundant genera with the experimental condition on the *x*-axis. Red squares indicate high abundance, whereas blue indicates lower abundance. When the genera were not known, the highest level of known classification is provided with the ASV number.

heatmaps show that the community composition differs among the three pipelines regarding the fungal community; however, the fungal community was similar among the biofilms. Several genera were more abundant in the water compared to the other environments, including an unidentified Rozellomycota, *Armillaria*, *Hypholoma*, and *Cortinarius*. The PCoA and PERMANOVA analyses show clear differences in the community composition among the pipelines ($F_{2,51} = 8.5$, $P < 0.001$; Figure 4A).

The different pipelines produced varying results between the experimental environments. For DADA2, Shannon diversity was greater in the water compared to the floating leaves ($F_{1,9} = 14.3$, $P = 0.0042$), and based on PERMANOVA analysis, there was no difference in the community composition between environments ($F_{1,10} = 0.64$, $P = 0.53$), but these results differed among plant species ($F_{1,10} = 1.2$, $P = 0.02$; Appendix S7). However, neither Deblur nor UNOISE identified differences in ASV richness or Shannon diversity nor differences in the community composition between environments or between plant species (Appendix S7).

Little variation in predicted 18S rRNA community composition among pipelines

For the 18S rRNA mock community, Deblur identified the fewest sequences, whereas DADA2 and UNOISE performed similarly (Appendix S3E); however, this difference was not statistically significant ($F_{2,36} = 1.02$, $P = 0.37$). DADA2 and UNOISE also identified similar genera with similar relative abundances, unlike Deblur (Appendix S3F). Thus, it is

expected that the environmental data will have similar results between DADA2 and UNOISE. Upon removing the ASVs with no taxonomic information, the total number of ASVs was similar among the three pipelines: DADA2 (534), Deblur (483), and UNOISE (501), which differs from the dominance of UNOISE observed in the other domain analyses (Appendix S5).

For the environmental samples, UNOISE detected the most reads but DADA2 and Deblur better represented the overall richness (Appendix S4C). Similar to 16S rRNA and ITS rRNA, there is a difference in ASV richness among pipelines (Appendix S5) for 18S rRNA community composition ($F_{2,33} = 20.9$, $P < 0.001$). Upon removing the ASVs with no taxonomic information, the total number of ASVs varied among the three pipelines: DADA2 (534), Deblur (483), and UNOISE (501), although this differs from the dominance of UNOISE observed in the other domain analyses (Appendix S5, Figure 5). There was no difference in Shannon diversity or community composition among the pipelines (Appendix S8).

There are several differences in the relative abundance of phyla between floating and submerged biofilms, with Orchophyta ($F_{1,34} = 4.1$, $P = 0.05$), Peronosporomycetes ($F_{1,34} = 9.4$, $P = 0.004$), Cercozoa ($F_{1,34} = 7.0$, $P = 0.01$), Gastrotricha ($F_{1,34} = 4.5$, $P = 0.04$), Cryptophyceae ($F_{1,34} = 6.4$, $P = 0.02$), Protalveolata ($F_{1,34} = 4.2$, $P = 0.04$), and Bicosoecida ($F_{1,34} = 8.9$, $P = 0.005$) all found to be more abundant on the submerged leaves compared to the floating leaves. Despite differences at the phylum level, likely driven by taxa with low abundance, the most abundant genera were found to be similar among pipelines. Cryptomycota and *Podocopidia* were more abundant in the floating leaf biofilms but were also detected in high abundance in both floating and submerged leaves and in all three pipelines. Each pipeline detected three different Embryophyta ASVs, and these were more abundant in the submerged leaf biofilms. The nematode Chromadorida was more abundant in the floating leaves. Moreover, the PCoA and PERMANOVA analyses show the clustering of the pipelines (Figure 6A) with a significant difference in community composition among pipelines ($F_{2,33} = 12.1$, $P < 0.001$; Appendix S5). Based on the heatmap, each pipeline identified at least two different ASVs of Embryophyta, one of which was more abundant in the submerged leaves and the other more abundant in the floating leaves (Figure 6B). A total of 65% of the genera were shared among all the pipelines, and Deblur identified the

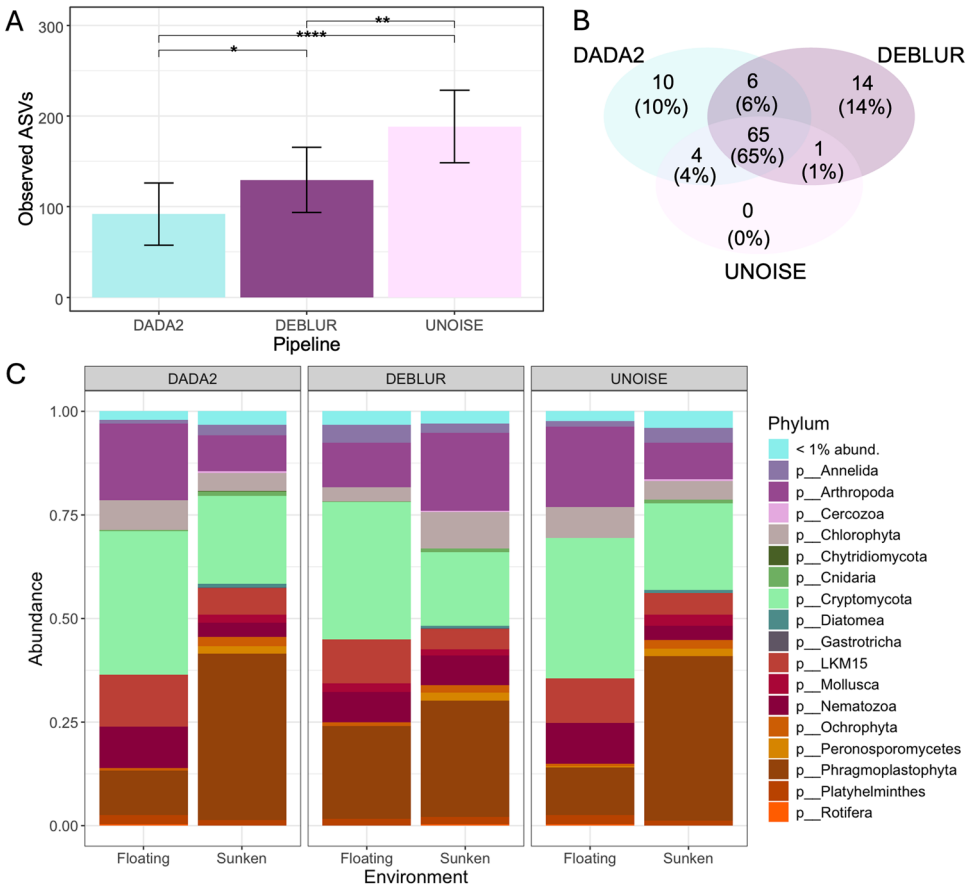

FIGURE 5 Alpha diversity of microeukaryotic communities. (A) Microeukaryotic ASV richness for each experimental condition as determined by each denoising pipeline. The height of the bar represents the mean, and the bars are the standard deviation. Statistical differences in the number of ASVs detected by each pipeline determined by a *t*-test are noted with * ($P < 0.05$), ** ($P < 0.01$), and **** ($P < 0.0001$). (B) Venn diagram showing the number (and percentage) of microeukaryotic genera unique to each pipeline and shared among them. (C) Stacked-bar plot showing the relative abundance of microeukaryotic phyla (p__) identified from each pipeline and environment.

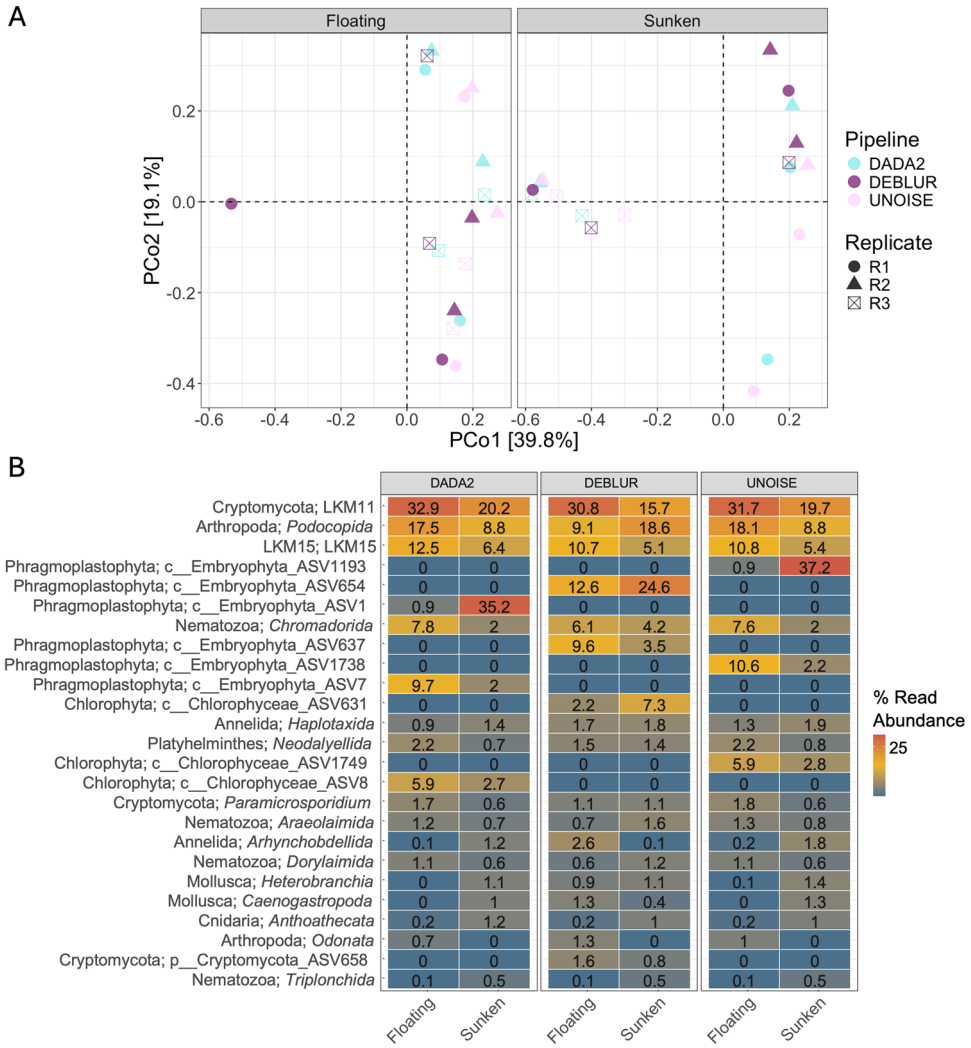

FIGURE 6 Microeukaryotic microbial community composition. (A) PCoA plot of the eukaryotic community composition according to the experimental treatment. The colors represent the three pipelines, and the shapes represent the replicates. If the replicates from each pipeline are similar to each other, then they share a similar community composition. The *y*-axis is the same for each experimental condition and shows that the microbial community composition was similar across all experimental conditions. (B) Heatmap divided by pipeline showing the 25 most abundant genera with the experimental condition on the *x*-axis. Red squares indicate high abundance, whereas blue indicates lower abundance. When the genera were not known, the highest level of known classification is provided with the ASV number.

greatest number of unique genera ($n = 14$; Figure 5B), although UNOISE detected more Holozoa than Deblur ($F_{2,33} = 4.6$, $P = 0.013$).

DISCUSSION

The results obtained by the three methods (DADA2, Deblur, and UNOISE) with the 16S rRNA (bacteria), ITS rRNA (fungi), and 18S rRNA (nonfungal eukaryotes) datasets were compared to determine changes in alpha and beta diversity among the pipelines. Although the sets of biofilm samples used in each pipeline were the same, dissimilarities in the results can lead to different conclusions regarding the microbial community. This was further confirmed using mock communities. Furthermore, we highlighted how these data can be interpreted from a plant taphonomic viewpoint.

The mock community analysis shows that each pipeline can provide results that differ in community composition and in the overall read abundance. Additionally, as we observed differences in the patterns of the mock community compared to the biofilm samples, the effectiveness of each pipeline is dependent on the individual dataset. Thus, the potential biases posed by each pipeline should be considered when interpreting the results of any sequencing study.

Pipelines with 16S rRNA highlight the trade-off between high sequence abundance and taxonomic identification

Using the biofilm samples, we found that UNOISE (via VSEARCH) was the most effective tool for identifying the

highest number of 16S rRNA ASVs, while DADA2 and Deblur produced similarly lower counts of ASVs (Figure 1A). However, a greater number of ASVs does not necessarily mean that UNOISE performed better, as the resulting taxonomy should also be assessed. A greater number of ASVs could also be explained by the occurrence of "artificial" species resulting from the splitting of taxonomic groups (Schloss, 2021). The discrepancy between UNOISE and DADA2 could be due to the more accurate error-detection rates of DADA2 (Bukin et al., 2023). Therefore, in some studies, the count table of ASVs observed in DADA2 and UNOISE were combined in the consensus table to minimize erroneous and low abundant ASVs (Modin et al., 2020; Karačić et al., 2022).

Previous studies have observed lower ASV counts using Deblur compared to both DADA2 and UNOISE (Prodan et al., 2020). Although all three methodologies identified the same 515 genera, making up 48% of the total, DADA2 was notable for identifying the greatest number of unique genera (Figure 1B). This could again be attributed to DADA2's enhanced error-correction abilities, which likely improved its matching of ASVs to known taxa in the database. Previous work analyzing such denoising methods for fecal microbiomes found similar discrepancies in the identified genera among the pipelines (Liu et al., 2023). On the other hand, Deblur might have identified fewer genera because it eliminates sequences appearing fewer than 10 times, in contrast to DADA2, which removes sequences that occur only once (Callahan et al., 2016; Amir et al., 2017). The removal of such sequences eliminates sequences that may be artifacts instead of microbial taxa; however, with its higher removal rate, Deblur may not detect as many rare taxa, which can be important to the function and structure of the microbial communities (Shade et al., 2014). Each method thus employs a strategy to discard single-occurrence sequences and those with low frequencies, which helps eliminate some errors but also inadvertently removes rare taxa. Researchers should choose their threshold levels carefully to ensure they best fit their objectives.

Upon comparing genus-level microbial community composition across pipelines, each pipeline identified the same abundant genera, leading to broadly similar microbial community profiles (Figure 2). This suggests that, despite the pipelines identifying distinct genera (Figure 1), the discrepancies mainly occur among genera with low relative abundance. However, many studies observed that the ASV approach used by DADA2 has a higher precision for detecting rare taxa (He et al., 2015; Modin et al., 2020).

Overall community composition at the genus level remains comparable across the pipelines, with all three identifying the same highly abundant genera. The abundance of Alphaproteobacteria varied among the pipelines. This is important to note when assessing the microbial community composition of biofilms, as Alphaproteobacteria is often the most abundant class of bacteria during early biofilm formation (Rehman et al., 2020). Our results suggest that either UNOISE can better detect Alphaproteobacteria sequences or, due to the high number of total ASVs, the number of Alphaproteobacteria sequences may be inflated. Prokaryotic community composition and richness also differed between depths. The genera that were more abundant on the submerged leaves include the biofilm-forming and occasionally pathogenic *Pseudomonas* (Tolker-Nielsen et al., 2000; Höfte and De Vos, 2006), while *Novosphingobium*, a genus found in a variety of different environments (Kumar et al., 2017), and the biofilm-forming plant pathogen *Panteoa* (Von Bodman et al., 2003) were more abundant on the floating leaves.

Results from ITS sequences highlight the importance of pipeline selection

Interestingly, we did not observe the same patterns among the pipelines when using the ITS region dataset, which had a lower overall count of ASVs that could have made the results less stable. The UNITE database is less robust than Silva v138, and fungal communities are not as diverse as bacterial communities; thus, we can expect a difference in the ASV richness between the 16S rRNA and the ITS region. There were a few differences at the phylum level among the pipelines, the most notable being the identification of more Ascomycota by Deblur. Most of the differences in the relative abundances of phyla were specific to the surrounding environment (water vs. soil) and their related biofilms rather than resulting from the choice of pipeline. The fungal community also differed between plant species, although only when the DADA2 pipeline was used.

Contrary to the 16S rRNA analyses, Deblur identified the greatest number of ASVs and had the most unique genera, with only 14 genera identified by all three pipelines. These discrepancies in ITS data could come from differences in ASV/operational taxonomic unit (OTU) length or robust clustering processes in which short reads were covered by longer reads that were merged in the centroid OTU for UNOISE (Modin et al., 2020; Rolling et al., 2022). However, UNOISE is very good at identifying highly abundant sequences, which could explain a higher number of identified Basidiomycetes. Recent research also showed that OTUs were better than ASVs in recovering fungal diversity (Tedersoo et al., 2022).

The differences at the phylum level are also found at the genus level, where the PERMANOVAs show differences in the microbial community composition among the pipelines. This could be because of the lower number of ASVs identified using UNITE, which could place a greater emphasis on the differences in rare taxa detected by each pipeline (Nearing et al., 2018). Therefore, we suggest that additional fungal mock communities should be analyzed in parallel with plant samples in future studies to better explore these issues.

Denoising pipelines perform similarly for 18S eukaryotes

The denoising pipelines yielded similar results for the 18S rRNA sequences. Like 16S rRNA, UNOISE identified the

highest number of ASVs, although the 18S rRNA dataset had the highest percentage of genera shared among the pipelines (65%; Figure 5). The most abundant genera were similar among pipelines and the overall community composition, likely because of the above-mentioned reasons regarding 16S rRNA sequences. Previous work has shown that in microeukaryotic and phytoplankton communities, UNOISE yields greater richness than DADA2 (Bukin et al., 2023), which agrees with the results found in this study. However, in a soil nematode study, DADA2 outperformed Deblur, which was not the case observed here (Kenmotsu et al., 2020). This highlights the results we found when comparing the mock communities with the biofilm communities: the effectiveness of each pipeline is largely dependent on the study system. Therefore, if the time and resources are available, it is best to test multiple pipelines before drawing conclusions regarding microbial community composition.

The only phylum-level discrepancy among the pipelines with the 18S sequences was Holozoa, which was more commonly detected by UNOISE than Deblur. Holozoa is a broad taxonomic group, and the difference among denoising methods is likely a result of a greater number of sequences detected by UNOISE overall. Other phyla, however, did not differ among pipelines but differed between the environments, shedding light on how the environment can shape microeukaryotic communities within a biofilm. Ochrophyta contain brown algae and diatoms, which were more abundant on the submerged leaves. Diatoms, and the extracellular substances they produce, are thought to be an important aspect of soft-tissue preservation via biofilms (Harding and Chant, 2000). Cercozoa consist of single-celled eukaryotes and are important constituents of freshwater food webs as natural predators of bacteria (Šimek et al., 2020). They were more abundant on the submerged leaves, which contained a greater number and higher diversity of bacteria. Gastrotricha are primarily benthic, which is why they were more abundant on the submerged leaves (Strayer et al., 2010). The freshwater alga in Cryptophyceae (Klaveness, 1989), the protists in Protalveolata (Cavalier-Smith, 1993), and flagellate Bicosoecida (Metz et al., 2022) were also more abundant on the submerged leaves.

Taxonomic domain is an important factor in denoising pipeline selection

Given the results presented, researchers should be aware of the bias in results that are produced by each pipeline and choose a pipeline based on careful consideration of the objectives of their analyses. Additionally, it is important to compare results from different pipelines to interpret the data, due to biases of the different pipelines targeting abundant or rare genera. For bacteria (16S) and nonfungal eukaryotes (18S), DADA2 performed the best based on both the number of sequences detected and the ability to taxonomically identify them with Silva v138. Although UNOISE detected more sequences, it is important to consider the lack of taxonomic information associated with UNOISE for this group of environmental samples. For the fungal communities (ITS), there were differences in the number of detected sequences among the pipelines, but DADA2 and Deblur identified the most taxa. We recommend either DADA2 or Deblur, as they were more similar in their community composition and are likely a better representation of the true fungal community. If researchers can use the 99% UNITE database or another database to classify the fungi, such as NCBI Blast, it may decrease the number of ASVs but increase the reliability of the true fungal community composition.

The environmental conditions influence the biofilm microbial community composition

Once the appropriate denoiser is chosen, differences in the patterns of community assembly among bacteria, fungi, and microeukaryotes could be driven by environmental conditions. In our study, it is apparent that the bacterial community is influenced by the depth from which the water lily leaves had been recovered. On the floating leaves, bacteria are either derived from the surrounding environment (air and water) or the plant. These leaves are also exposed to a markedly different environment, and the lower bacterial abundance could be due to exposure to ultraviolet light (Jacobs and Sundin, 2001). When the leaves sink and environmental conditions change, the bacterial and microeukaryotic communities also shift in response to differences in oxygenation and light availability. The fungal community is not as affected by the modifications in environmental conditions at greater depth; fungi may be less impacted by environmental alterations because they are not photosynthetic. Furthermore, as these leaves were collected from a seminatural environment (a botanic garden pond), there is uncertainty of how long the submerged leaves were in the mud, thus introducing another variable potentially affecting the microbial community composition. Future work will use laboratory experiments with consistent leaf-burial conditions to address this question. Our study thus yields evidence for domain-stratified responses to depth-induced changes in environmental conditions, as is shown in previous studies with different organisms (Pang et al., 2016; Li et al., 2021).

CONCLUSIONS

The integration of next-generation sequencing techniques in experimental taphonomy represents a significant advancement in our understanding of the microbial communities involved in decay processes. Here, we highlight the importance of using appropriate methodologies for microbiological studies of plant decay and preservation by comparing results produced by different pipelines based on a

taphonomic dataset. Based on our results, we recommend DADA2 for 16S rRNA and 18S rRNA analyses due to its robust error-detection capabilities and its ability to identify more genera, including potentially rare taxa. While the choice of pipeline for analysis of the ITS region presents a more nuanced decision, Deblur detected the greatest number of ASVs, although these results were compositionally similar to DADA2. Either DADA2 or Deblur could be appropriate for fungal analyses. These findings contribute to bridging the gap between plant taphonomy and microbiology, paving the way for further exploration into the intricate role of microbes in plant decay and preservation.

The next-generation sequencing of plant samples also allowed us to conclude that microbial biofilm communities are involved in the initial stages of water lily decay. Biofilms on decaying floating and submerged water lily leaves contain different microbial communities, with bacteria and microeukaryotes varying by depth. During decay, as the water lily leaf sinks to the pond bottom, the biofilm microbial community shifts and, in the process, alters the decay and preservation processes. Future research should address further decay and preservation processes using controlled experimental design and targeted application of specific pipelines to understand which microbes are responsible for decay or biomineralization processes that could lead to preservation.

AUTHOR CONTRIBUTIONS

B.P. and S.K. performed sample preparation, DNA extraction, and data analysis. B.P. wrote the manuscript with contributions from S.K., C.T.G., and G.B. B.P. collected the samples. S.K. and G.B. contributed to the data analysis. C.T.G. and B.P. conceived and designed the initial study collecting water lily leaves. B.P. and S.K. conceived the bioinformatics aspects of the study. C.T.G. provided funding. All authors approved the final version of the manuscript.

ACKNOWLEDGMENTS

The authors sincerely thank Dr. Cornelia Löhne and Felix Eisenhuth (Bonn University Botanic Garden) for access to and assistance with collecting water lily leaves. This is contribution number 64 of the Deutsche Forschungsgemeinschaft (DFG) Research Unit FOR 2685 "The Limits of the Fossil Record: Analytical and Experimental Approaches to Fossilization" (project number 348043586, grant numbers GE 751/7-1 and GE 751/6-1 to C.T.G.). The authors also thank the two reviewers and the editor who read the early version of this manuscript. Thanks to their contributions, this study is much improved. Open Access funding enabled and organized by Projekt DEAL.

CONFLICT OF INTEREST STATEMENT

C.T.G. is an associate editor of *Applications in Plant Sciences* but took no part in the peer-review and decision-making processes for this paper.

DATA AVAILABILITY STATEMENT

All sequences and raw data are available through the National Center for Biotechnology Information (NCBI) under BioProject number PRJNA1043867 (http://www.ncbi.nlm.nih.gov/bioproject/1043867).

ORCID

Brianne Palmer https://orcid.org/0000-0002-4940-2719
Sabina Karačić https://orcid.org/0000-0003-0440-2456
Gabriele Bierbaum https://orcid.org/0000-0002-2933-8473
Carole T. Gee https://orcid.org/0000-0001-5926-2556

REFERENCES

Allali, I., J. W. Arnold, J. Roach, M. B. Cadenas, N. Butz, H. M. Hassan, M. Koci, et al. 2017. A comparison of sequencing platforms and bioinformatics pipelines for compositional analysis of the gut microbiome. *BMC Microbiology* 17: 194.

Amir, A., D. McDonald, J. A. Navas-Molina, E. Kopylova, J. T. Morton, Z. Zech Xu, E. P. Kightley, et al. 2017. Deblur rapidly resolves single-nucleotide community sequence patterns. *mSystems* 2: e00191–e00216.

Andersen, K. S., R. H. Kirkegaard, S. M. Karst, and M. Albertsen. 2018. ampvis2: An R package to analyse and visualise 16S rRNA amplicon data. *BioRxiv*: 299537 [Preprint]. Available at: https://doi.org/10.1101/299537 [posted 11 April 2018; accessed 5 December 2024].

Bakker, M. G. 2018. A fungal mock community control for amplicon sequencing experiments. *Molecular Ecology Resources* 18: 541–556.

Bolyen, E., J. R. Rideout, M. R. Dillon, N. A. Bokulich, C. C. Abnet, G. A. Al-Ghalith, H. Alexander, et al. 2019. Reproducible, interactive, scalable and extensible microbiome data science using QIIME 2. *Nature Biotechnology* 37: 852–857.

Bradley, I. M., A. J. Pinto, and J. S. Guest. 2016. Design and evaluation of Illumina MiSeq-compatible, 18S rRNA gene-specific primers for improved characterization of mixed phototrophic communities. *Applied and Environmental Microbiology* 82: 5878–5891.

Bukin, Y. S., I. S. Mikhailov, D. P. Petrova, Y. P. Galachyants, Y. R. Zakharova, and Y. V. Likhoshway. 2023. The effect of metabarcoding 18S rRNA region choice on diversity of microeukaryotes including phytoplankton. *World Journal of Microbiology and Biotechnology* 39: 229.

Callahan, B. J., P. J. McMurdie, M. J. Rosen, A. W. Han, A. J. A. Johnson, and S. P. Holmes. 2016. DADA2: High resolution sample inference from Illumina amplicon data. *Nature Methods* 13: 581–583.

Caporaso, J. G., C. L. Lauber, W. A. Walters, D. Berg-Lyons, C. A. Lozupone, P. J. Turnbaugh, N. Fierer, and R. Knight. 2011. Global patterns of 16S rRNA diversity at a depth of millions of sequences per sample. *Proceedings of the National Academy of Sciences, USA* 108: 4516–4522.

Cavalier-Smith, T. 1993. Kingdom protozoa and its 18 phyla. *Microbiological Reviews* 57: 953–994.

Choi, T.-J., A. Malik, H.-E. An, J.-I. Kim, T. Dinh Do, and C.-B. Kim. 2022. Seasonal diversity of microeukaryotes in the Han River, Korea through 18S rRNA gene metabarcoding. *Evolutionary Bioinformatics* 18: 11769343221074688.

Dhami, N., P. Greenwood, S. Poropat, M. Tripp, A. Elson, H. Vijay, L. Brosnan, et al. 2023. Microbially mediated fossil concretions and their characterization by the latest methodologies: A review. *Frontiers in Microbiology* 14: 1225411.

Dong, B., R. Han, and G. Wang. 2017. Research advances in and perspectives on characteristics of the micro-boundary layer around leaves and stems of submerged macrophytes. *Acta Ecologica Sinica* 37: 1769–1776.

Donlan, R. M. 2002. Biofilms: Microbial life on surfaces. *Emerging Infectious Diseases* 8: 881.

Dowd, S. E., R. D. Wolcott, Y. Sun, T. McKeehan, E. Smith, and D. Rhoads. 2008. Polymicrobial nature of chronic diabetic foot ulcer biofilm infections determined using bacterial tag encoded FLX amplicon pyrosequencing (bTEFAP). *PLoS ONE* 3: e3326.

Edgar, R. C. 2016. UNOISE2: Improved error-correction for Illumina 16S and ITS amplicon sequencing. *BioRxiv*: 081257 [Preprint]. Available at: https://doi.org/10.1101/081257 [posted 15 October 2016; accessed 5 December 2024].

Gee, C. T. 1996. Plant taphonomy and actuopaleobotany in NW Europe: Proceedings of the 6th International Workshop on Plant Taphonomy in Bonn, 12 November 1994. Neues Jahrbuch für Geologie und Paläontologie–Abhandlungen: 143–148.

Harding, I. C., and L. S. Chant. 2000. Self-sedimented diatom mats as agents of exceptional fossil preservation in the Oligocene Florissant lake beds, Colorado, United States. *Geology* 28: 195–198.

He, D., L. Ren, and Q. Wu. 2012. Epiphytic bacterial communities on two common submerged macrophytes in Taihu Lake: Diversity and host-specificity. *Chinese Journal of Oceanology and Limnology* 30: 237–247.

He, D., L. Ren, and Q. L. Wu. 2014. Contrasting diversity of epibiotic bacteria and surrounding bacterioplankton of a common submerged macrophyte, *Potamogeton crispus*, in freshwater lakes. *FEMS Microbiology Ecology* 90: 551–562.

He, Y., J. G. Caporaso, X.-T. Jiang, H.-F. Sheng, S. M. Huse, J. R. Rideout, R. C. Edgar, et al. 2015. Stability of operational taxonomic units: An important but neglected property for analyzing microbial diversity. *Microbiome* 3: 20.

Höfte, M., and P. De Vos. 2006. Plant pathogenic *Pseudomonas* species. *In* S. S. Gnanamanickam [ed.], Plant-associated bacteria, 507–533. Springer, Dordrecht, the Netherlands.

Iniesto, M., I. Villalba, A. D. Buscalioni, M. C. Guerrero, and A. I. López-Archilla. 2017. The effect of microbial mats in the decay of anurans with implications for understanding taphonomic processes in the fossil record. *Scientific Reports* 7: 45160.

Iniesto, M., C. Blanco-Moreno, A. Villalba, Á. D. Buscalioni, M. C. Guerrero, and A. I. López-Archilla. 2018. Plant tissue decay in long-term experiments with microbial mats. *Geosciences* 8: 387.

Iniesto, M., P. Gutiérrez-Silva, J. J. Dias, I. S. Carvalho, A. D. Buscalioni, and A. I. López-Archilla. 2021. Soft tissue histology of insect larvae decayed in laboratory experiments using microbial mats: Taphonomic comparison with Cretaceous fossil insects from the exceptionally preserved biota of Araripe, Brazil. *Palaeogeography, Palaeoclimatology, Palaeoecology* 564: 110156.

Jacobs, J. L., and G. W. Sundin. 2001. Effect of solar UV-B radiation on a phyllosphere bacterial community. *Applied and Environmental Microbiology* 67: 5488–5496.

Janssen, K., S. L. Low, Y. Wang, Q.-Y. Mu, G. Bierbaum, and C. T. Gee. 2021. Elucidating biofilm diversity on water lily leaves through 16S rRNA amplicon analysis: Comparison of four DNA extraction kits. *Applications in Plant Sciences* 9: e11444.

Janssen, K., B. Mähler, J. Rust, G. Bierbaum, and V. E. McCoy. 2022. The complex role of microbial metabolic activity in fossilization. *Biological Reviews* 97: 449–465.

Karačić, S., O. Modin, P. Hagelia, F. Persson, and B.-M. Wilén. 2022. The effect of time and surface type on the composition of biofilm communities on concrete exposed to seawater. *International Biodeterioration and Biodegradation* 173: 105458.

Karačić, S., B. Palmer, C. T. Gee, and G. Bierbaum. 2024. Oxygen-dependent biofilm dynamics in leaf decay: An in vitro analysis. *Scientific Reports* 14: 6728.

Kaye, T. G., G. Gaugler, and Z. Sawlowicz. 2008. Dinosaurian soft tissues interpreted as bacterial biofilms. *PLoS ONE* 3: e2808.

Kenmotsu, H., K. Uchida, Y. Hirose, and T. Eki. 2020. Taxonomic profiling of individual nematodes isolated from copse soils using deep amplicon sequencing of four distinct regions of the 18S ribosomal RNA gene. *PLoS ONE* 15: e0240336.

Klaveness, D. 1989. Biology and ecology of the Cryptophyceae: Status and challenges. *Biological Oceanography* 6: 257–270.

Knauth, S., H. Schmidt, and R. Tippkötter. 2013. Comparison of commercial kits for the extraction of DNA from paddy soils. *Letters in Applied Microbiology* 56: 222–228.

Korabecná, M., V. Liska, and K. Fajfrlík. 2003. Primers ITS1, ITS2 and ITS4 detect the intraspecies variability in the internal transcribed spacers and 5.8S rRNA gene region in clinical isolates of fungi. *Folia Microbiologica* 48: 233–238.

Kumar, R., H. Verma, S. Haider, A. Bajaj, U. Sood, K. Ponnusamy, S. Nagar, et al. 2017. Comparative genomic analysis reveals habitat-specific genes and regulatory hubs within the genus *Novosphingobium*. *mSystems* 2: e00020-17.

Lear, G., A. Dopheide, P.-Y. Ancion, K. Roberts, V. Washington, J. Smith, and G. D. Lewis. 2012. Biofilms in freshwater: Their importance for the maintenance and monitoring of freshwater health. *In* G. Lear and G. D. Lewis [eds.], Microbial biofilms: Current research and applications, 129–151. Caister Academic Press, Poole, United Kingdom.

Lee, E.-S., S.-Y. Cha, and J.-S. Jung. 2021. Evaluation of DNA extraction methods for quantifying *Helicobacter pylori* in water with PCR inhibitors. *Water Supply* 21: 4525–4533.

Letáková, M., M. Fránková, and A. Poulíčková. 2018. Ecology and applications of freshwater epiphytic diatoms. *Cryptogamie, Algologie* 39: 3–22.

Li, H., Y. Li, D. Huang, L. Zhang, J. Lu, and J. Zhang. 2021. The response mechanism of *Hydrilla verticillata* and leaf epiphytic biofilms to depth and nutrient removal. *Environmental Science and Pollution Research* 28: 49032–49041.

Liu, C., Y. Cui, X. Li, and M. Yao. 2021. microeco: An R package for data mining in microbial community ecology. *FEMS Microbiology Ecology* 97: fiaa255.

Liu, G., T. Li, X. Zhu, X. Zhang, and J. Wang. 2023. An independent evaluation in a CRC patient cohort of microbiome 16S rRNA sequence analysis methods: OTU clustering, DADA2, and Deblur. *Frontiers in Microbiology* 14: 1178744.

Mähler, B., K. Janssen, M. Tahoun, F. Tomaschek, R. Schellhorn, C. E. Müller, G. Bierbaum, and J. Rust. 2022. Adipocere formation in biofilms as a first step in soft tissue preservation. *Scientific Reports* 12: 10122.

Mähler, B., K. Janssen, M. I. Lönartz, M. Lagos, T. Geisler, J. Rust, and G. Bierbaum. 2023. Time-dependent microbial shifts during crayfish decomposition in freshwater and sediment under different environmental conditions. *Scientific Reports* 13: 1539.

Metz, S., P. Huber, V. Accattatis, A. Lopes dos Santos, E. Bigeard, F. Unrein, A. Chambouvet, et al. 2022. Freshwater protists: Unveiling the unexplored in a large floodplain system. *Environmental Microbiology* 24: 1731–1745.

Modin, O., R. Liébana, S. Saheb-Alam, B.-M. Wilén, C. Suarez, M. Hermansson, and F. Persson. 2020. Hill-based dissimilarity indices and null models for analysis of microbial community assembly. *Microbiome* 8: 132.

Nearing, J. T., G. M. Douglas, A. M. Comeau, and M. G. I. Langille. 2018. Denoising the Denoisers: An independent evaluation of microbiome sequence error-correction approaches. *PeerJ* 6: e5364.

Nilsen, T., L.-G. Snipen, I. L. Angell, N. B. Keeley, S. Majaneva, R. Pettersen, and K. Rudi. 2024. Swarm and UNOISE outperform DADA2 and Deblur for denoising high-diversity marine seafloor samples. *ISME Communications* 4: ycae071.

Nilsson, R. H., K.-H. Larsson, A. F. S. Taylor, J. Bengtsson-Palme, T. S. Jeppesen, D. Schigel, P. Kennedy, et al. 2019. The UNITE database for molecular identification of fungi: Handling dark taxa and parallel taxonomic classifications. *Nucleic Acids Research* 47: D259–D264.

Pang, S., S. Zhang, X. Lv, B. Han, K. Liu, C. Qiu, C. Wang, et al. 2016. Characterization of bacterial community in biofilm and sediments of wetlands dominated by aquatic macrophytes. *Ecological Engineering* 97: 242–250.

Peterson, J. E., M. E. Lenczewski, and R. P. Scherer. 2010. Influence of microbial biofilms on the preservation of primary soft tissue in fossil and extant archosaurs. *PLoS ONE* 5: e13334.

Prodan, A., V. Tremaroli, H. Brolin, A. H. Zwinderman, M. Nieuwdorp, and E. Levin. 2020. Comparing bioinformatic pipelines for microbial 16S rRNA amplicon sequencing. *PLoS ONE* 15: e0227434.

Quast, C., E. Pruesse, P. Yilmaz, J. Gerken, T. Schweer, P. Yarza, J. Peplies, and F. O. Glöckner. 2013. The SILVA ribosomal RNA gene database project: Improved data processing and web-based tools. *Nucleic Acids Research* 41: D590–D596.

R Core Team. 2024. R: A language and environment for statistical computing. R Foundation for Statistical Computing, Vienna, Austria. Website: http://www.R-project.org/ [accessed 6 December 2024].

Raff, E. C., K. L. Schollaert, D. E. Nelson, P. C. J. Donoghue, C.-W. Thomas, F. R. Turner, B. D. Stein, et al. 2008. Embryo fossilization is a biological process mediated by microbial biofilms. *Proceedings of the National Academy of Sciences, USA* 105: 19360–19365.

Rehman, Z. U., L. Fortunato, T. Cheng, and T. Leiknes. 2020. Metagenomic analysis of sludge and early-stage biofilm communities of a submerged membrane bioreactor. *Science of the Total Environment* 701: 134682.

Rognes, T., T. Flouri, B. Nichols, C. Quince, and F. Mahé. 2016. VSEARCH: A versatile open source tool for metagenomics. *PeerJ* 4: e2584.

Rolling, T., B. Zhai, J. Frame, T. M. Hohl, and Y. Taur. 2022. Customization of a DADA2-based pipeline for fungal internal transcribed spacer 1 (ITS1) amplicon data sets. *JCI Insight* 7: e151663.

Schloss, P. D. 2021. Amplicon sequence variants artificially split bacterial genomes into separate clusters. *mSphere* 6: e0019121.

Shade, A., S. E. Jones, J. G. Caporaso, J. Handelsman, R. Knight, N. Fierer, and J. A. Gilbert. 2014. Conditionally rare taxa disproportionately contribute to temporal changes in microbial diversity. *MBio* 5: e01371-14.

Šimek, K., V. Grujčić, I. Mukherjee, V. Kasalický, J. Nedoma, T. Posch, M. Mehrshad, and M. M. Salcher. 2020. Cascading effects in freshwater microbial food webs by predatory Cercozoa, Katablepharidacea and ciliates feeding on aplastidic bacterivorous cryptophytes. *FEMS Microbiology Ecology* 96: fiaa121.

Strayer, D. L., W. D. Hummon, and R. Hochberg. 2010. Chapter 7: Gastrotricha. *In* J. H. Thorp and A. P. Covich [eds.], Ecology and classification of North American freshwater invertebrates, 3rd ed., 163–172. Academic Press, New York, New York, USA.

Tedersoo, L., M. Bahram, L. Zinger, R. H. Nilsson, P. G. Kennedy, T. Yang, S. Anslan, and V. Mikryukov. 2022. Best practices in metabarcoding of fungi: From experimental design to results. *Molecular Ecology* 31: 2769–2795.

Tolker-Nielsen, T., U. C. Brinch, P. C. Ragas, J. B. Andersen, C. S. Jacobsen, and S. Molin. 2000. Development and dynamics of *Pseudomonas* sp. biofilms. *Journal of Bacteriology* 182: 6482–6489.

Toporski, J. K. W., A. Steele, F. Westall, R. Avci, D. M. Martill, and D. S. McKay. 2002. Morphologic and spectral investigation of exceptionally well-preserved bacterial biofilms from the Oligocene Enspel formation, Germany. *Geochimica et Cosmochimica Acta* 66: 1773–1791.

Von Bodman, S., M. Koutsoudis, and T. Minogue. 2003. Steps in biofilm formation and infection in *Pantoea stewartii* subsp. *stewartii*. *Phytopathology* 92: S97.

SUPPORTING INFORMATION

Additional supporting information can be found online in the Supporting Information section at the end of this article.

Appendix S1. Schematic of the generalized steps of each denoising pipeline.

Appendix S2. Denoiser code.

Appendix S3. Results from the mock community analysis.

Appendix S4. Rarefaction curves showing the sequencing depth and the number of observed ASVs for each sample.

Appendix S5. Denoiser ASV count.

Appendix S6. 16S observed ASVs and Shannon diversity.

Appendix S7. ITS observed ASVs and Shannon diversity.

Appendix S8. 18S observed ASVs and Shannon diversity.

How to cite this article: Palmer, B., S. Karačić, G. Bierbaum, and C. T. Gee. 2025. Microbial methods matter: Identifying discrepancies between microbiome denoising pipelines using a leaf biofilm taphonomic dataset. *Applications in Plant Sciences* 13(2): e11628. https://doi.org/10.1002/aps3.11628